Fluctuation-Induced Cross-Field Electron Transport and Dynamo Effect Accompanied by Turbulent Diffusion in an Electron Beam-Plasma System

R. Sugaya, T. Maehara and M. Sugawa

Department of Physics, Faculty of Science, Ehime University
Bunkyo-cho 2-5, Matsuyama 790-8577, Japan

Abstract

It has been proved theoretically and numerically that the cross-field electron transport and dynamo effect accompanied by turbulent diffusion are induced by the unstable localized electrostatic waves in an electron beam-plasma system.

1. Introduction

Fluctuation-induced cross-field electron transport and dynamo effect accompanied by turbulent diffusion in an electron beam-plasma system were investigated theoretically and numerically on the basis of the transport equations and magnetohydrodynamic equations[1-4]. It was verified that in the first stage where the unstable localized electrostatic waves are growing linearly or nonlinearly the cross-field electron transport and the generation of cross-field electric field are dominant[4], and in the second stage where the electrostatic waves saturate in the amplitude the turbulent diffusion becomes dominant in the formation of the plasma profile. In the first stage the parallel and perpendicular electron transport generates a large and abrupt dip of the electron density and a strong peak of the electron temperature in the radial direction. Simultaneously the cross-field electric field is produced partially by the cross-field electron transport and partially by the perpendicular pressure gradient, that is, it is given by $\boldsymbol{E}_\perp = \boldsymbol{B}_0 \times \boldsymbol{v}_{e\perp}/c - (\boldsymbol{\nabla}_\perp p_{e\perp})/en_e \ (p_e = n_e k_B T_e)$. The small cross-field electron transport is predicted to create the strong cross-field electric field. On the other hand, the parallel electric field $\boldsymbol{E}_\parallel = -(\boldsymbol{\nabla}_\parallel p_e)/en_e + m_e \nu_{en} \boldsymbol{v}_{e\parallel}/e$ is created by the parallel electron transport and the parallel ambipolar diffusion. Here, $\boldsymbol{B}_0 = (0,0,B_0)$ is the external magnetic field in the z direction, $\boldsymbol{v}_{e\perp} = (v_{ex}, v_{ey}, 0)$ is the cross-field drift velocity of plasma electrons, $\boldsymbol{v}_{e\parallel} = (0,0,v_{ez})$ is the parallel drift velocity of plasma electrons, and ν_{en} is the electron-neutral collision frequency. In the second stage the dip of the electron density, the peak of the electron temperature and the electric field vanish almost completely via the turbulent diffusion due to the large amplitude electrostatic waves. The radial and axial profiles of the electron density and temperature and the electric field were obtained numerically and they can explain well the experimental observation in an electron beam-plasma system qualitatively and quantitatively[5-7].

2. Transport Equations

We analyze the electron transport arising from due to spatially localized unstable electrostatic waves. The transport equations and magnetohydrodynamic equations for plasma electrons are expressed as

$$\frac{\partial U_e}{\partial t} = -2\gamma_{\boldsymbol{k}}^{(e)} U_{\boldsymbol{k}} \quad , \tag{1}$$

$$\frac{\partial \boldsymbol{P}_e}{\partial t} = -\frac{2\gamma_{\boldsymbol{k}}^{(e)} \boldsymbol{k}}{\omega_{\boldsymbol{k}}} U_{\boldsymbol{k}} - en_e \boldsymbol{E}_{\parallel} - \boldsymbol{\nabla}_{\parallel} p_e - m_e n_e \nu_{en} \boldsymbol{v}_{e\parallel} \quad , \tag{2}$$

$$n_e \boldsymbol{v}_{e\parallel} - \mu_e n_e \boldsymbol{E}_{\parallel} - \boldsymbol{\nabla}_{\parallel} (D_e n_e) = 0 \quad , \tag{3}$$

$$-en_e \boldsymbol{E}_{\perp} - (e/c) n_e \boldsymbol{v}_{e\perp} \times \boldsymbol{B}_0 - \boldsymbol{\nabla}_{\perp} p_e = 0 \quad , \tag{4}$$

$$\frac{\partial n_e}{\partial t} + \boldsymbol{\nabla} \cdot \boldsymbol{\Gamma}_e = 0 \quad , \tag{5}$$

$$\boldsymbol{\Gamma}_e = n_e \boldsymbol{v}_e - \mu_e n_e \boldsymbol{E}_{\parallel} - \boldsymbol{\nabla}_{\parallel} \left(D_e n_e + n_e v_{e\parallel}^2 / \nu_{en} \right) - \boldsymbol{\nabla}_{\perp} (D_a n_e) \quad , \tag{6}$$

$$\boldsymbol{\nabla} \cdot \boldsymbol{E} = 0 \quad , \tag{7}$$

where $U_{\boldsymbol{k}} = (1/8\pi)\left(\partial(\varepsilon'_{\boldsymbol{k}}\omega_{\boldsymbol{k}} / \partial\omega_{\boldsymbol{k}})\right)|E_{\boldsymbol{k}}|^2$ is the wave energy density, $\boldsymbol{k}U_{\boldsymbol{k}} / \omega_{\boldsymbol{k}}$ is the wave momentum density, $U_e = m_e n_e v_e^2 / 2 + 3n_e k_B T_e / 2$ and $\boldsymbol{P}_e = m_e n_e \boldsymbol{v}_e$ are the energy and momentum densities of plasma electrons, $\gamma_{\boldsymbol{k}}^{(e)}$ is the linear Landau and cyclotron damping rate ascribed to plasma electrons, $\mu_e = e / m_e \nu_{en}$ is the electron mobility, $D_e = k_B T_e / m_e \nu_{en}$ is the electron diffusion coefficient, $\varepsilon_{\boldsymbol{k}} = \varepsilon'_{\boldsymbol{k}} + i\varepsilon''_{\boldsymbol{k}}$ is the dielectric constant, and $\boldsymbol{k} = (k_{\perp}, 0, k_{\parallel})$. D_a shows the anomalous turbulent diffusion coefficient and it is assumed that $D_a = D_{a0} U_{\boldsymbol{k}} / U_{\boldsymbol{k}}(0)$ and $D_{a0} = \beta_a k_B T_{e0} / m_e \omega_{\boldsymbol{k}}$ ($\beta_a \sim 1$). Here, $U_{\boldsymbol{k}}(0)$ and T_{e0} are $U_{\boldsymbol{k}}$ and T_e at $t = 0$, $x, y, z = 0$, respectively. In Eq. (6), the mobility and the diffusion of plasma electrons across the magnetic field is neglected, namely $\mu_{e\perp}$ and $\boldsymbol{\nabla}_{\perp}\left(D_{e\perp} n_e + \left(\nu_{en} / \omega_{ce}^2\right) n_e v_{e\perp}^2\right)$ are neglected because of $\nu_{en} / \omega_{ce} \ll 1$ (ω_{ce} is the electron cyclotron frequency). On the other hand, Eq. (3) means that the diffusion along the magnetic field is the ambipolar diffusion. According to Eq. (3), the electron flux given by Eq. (6) is reduced to

$$\boldsymbol{\Gamma}_e = n_e \boldsymbol{v}_{e\perp} - \boldsymbol{\nabla}_{\perp} (D_a n_e) \quad , \tag{8}$$

under the condition of $D_e n_e \gg n_e v_{e\parallel}^2 / \nu_{en}$, and the transport equation (2) becomes

$$\frac{\partial \boldsymbol{P}_e}{\partial t} = -\frac{2\gamma_{\boldsymbol{k}}^{(e)} \boldsymbol{k}}{\omega_{\boldsymbol{k}}} U_{\boldsymbol{k}} - 2m_e n_e \nu_{en} \boldsymbol{v}_{e\parallel} \quad . \tag{9}$$

Equations (1) and (2) predict that the electrostatic waves create strong electron transport or acceleration along and across the magnetic field. The general Ohm's law of Eq. (4) shows that the cross-field electric field $\boldsymbol{E}_{\perp}$ is produced by the dynamo effect of the cross-field electron drift and the radial pressure gradient induced by the electron transport.

3. Numerical Analysis

The temporal and spatial development of the system has been investigated numerically assuming that the electrostatic waves excited in an electron-beam plasma system are localized radially such that $U_{\boldsymbol{k}} \propto \exp\left[-(x^2 + y^2)/a^2\right]$, and the background plasma is spatially uniform initially. Here a means the beam radius. The kinetic wave equations for electrostatic waves are assumed as follows:

$$\frac{\partial U_{\boldsymbol{k}}}{\partial t}=\left(2\gamma_{\boldsymbol{k}}^{(e)}+2\gamma_N e^{-2\gamma_{0b}t}\right)U_{\boldsymbol{k}},\quad \frac{\partial U_{\boldsymbol{k}}}{\partial z}=\left(2\gamma_i+2\gamma_{sN}e^{-2\gamma_0 z}\right)U_{\boldsymbol{k}} \quad . \tag{10}$$

The numerical analysis of Eqs. (1)-(10) was performed under the parameters of $\omega_{\boldsymbol{k}}/\omega_{ce}=0.3$, $k_\perp v_{te0}/\omega_{ce}=1$, $k_\parallel/k_\perp=0.2$, $\left|\gamma_{\boldsymbol{k}}^{(e)}\right|/\omega_{ce}=0.2$ ($\gamma_{\boldsymbol{k}}^{(e)}<0$), $\gamma_N/\left|\gamma_{\boldsymbol{k}}^{(e)}\right|=1.2$, $\gamma_{sN}v_{te0}/\left|\gamma_{\boldsymbol{k}}^{(e)}\right|=0.7$, $\gamma_{0b}v_{te0}/\left|\gamma_{\boldsymbol{k}}^{(e)}\right|=0.2$, $\gamma_0 v_{te0}/\left|\gamma_{\boldsymbol{k}}^{(e)}\right|=0.1$, $\gamma_1 v_{te0}/\gamma_{\boldsymbol{k}}^{(e)}=0.02$, $\gamma_2 v_{te0}/\gamma_{\boldsymbol{k}}^{(e)}=0.1$ ($\gamma_1,\gamma_2<0$), $v_{en}/\left|\gamma_{\boldsymbol{k}}^{(e)}\right|=0.8$, $a\omega_{ce}/v_{te0}=2$, $U_{\boldsymbol{k}}(0)/n_{e0}k_BT_{e0}=1.1\times10^{-4}$, $D_{a0}/\gamma_N a^2=0,\ 10^{-6}$, $\beta_a=1$, and $v_{te0}=\sqrt{k_BT_{e0}/m_e}$. In Eqs. (1) and (2), $\gamma_i=-\gamma_1$, and it is assumed that $\gamma_i=-\gamma_2$ in D_a in Eq. (6). Thus the temporal evolution of the three-dimensional profiles of the system was obtained. We show the only temporal evolutions of the transverse profiles in the x and y directions for the fixed value of $z\left|\gamma_{\boldsymbol{k}}^{(e)}\right|/v_{te0}=10$. Figure 1 exhibits the temporal evolutions of the transverse profiles without the anomalous turbulent diffusion due to the electrostatic waves, where $D_{a0}/\gamma_N a^2=0$, that is, n_e/n_{e0} and T_e/T_{e0} versus x/a and y/a are shown as a parameter of $\left|\gamma_{\boldsymbol{k}}^{(e)}\right|t=1$, 2 and 3 for the *x-y* profiles of (a), (b) and (c), respectively, where $n_{e0}=n_e(0)$ and $T_{e0}=T_e(0)$. It is found that the hollow profiles of the electron density and the peak profiles of the electron temperature develop temporally and axially (z direction). At the same time the cross-field electric field (not shown) is created. This means that the cross-field drift of plasma electrons (not shown) induced by the electrostatic waves generate the abrupt inhomogeneity of radial profile and the strong cross-field electric field. As was predicted in the previous work[4], the transport equations (1) and (2) govern v_{ex} and v_{ez}, and the generalized Ohm's law (4) shows that E_y is determined by v_{ex} and $\nabla_y p_e$. The axial electric field E_z is given by Eq. (3) and E_y and E_z produce E_x so as to satisfy the Poisson's equation (7). Thus E_x and $\nabla_x p_e$ create v_{ey} via $\boldsymbol{E}\times\boldsymbol{B}$ drift and the diamagnetic drift. Figure 2 is the temporal evolutions of the transverse profiles of n_e/n_{e0} and T_e/T_{e0} with the anomalous turbulent diffusion, where $D_{a0}/\gamma_N a^2=10^{-6}$ and $\left|\gamma_{\boldsymbol{k}}^{(e)}\right|t=1$, 2 and 3 for (a), (b) and (c). It can be seen that the hollow profiles of n_e and the peak profiles of T_e are suppressed significantly by the anomalous turbulent diffusion.

The typical parameters of the experiment reported by the author *et al.*[5-7] are $T_{e0}=5\,\mathrm{eV}$, $B_0=7\times10^{-3}\,\mathrm{T}$ and $a=1.5\times10^{-3}\,\mathrm{m}$, and hence $a\omega_{ce}/v_{te0}=2$ is satisfied. From the present numerical analysis (Fig. 2), we find that $\boldsymbol{v}_e/v_{te0}=(0.02,0.02,0.01)$ and $e\boldsymbol{E}a/k_BT_{e0}=$ (0.2,0.2,0.001) at $\left|\gamma_{\boldsymbol{k}}^{(e)}\right|t=$ 2. Thus, we obtain $\boldsymbol{E}a=(1,1,0.005)\,\mathrm{V}$, $Ea=1.4\,\mathrm{V}$, $\boldsymbol{E}$=(6.7×10^2, 6.7×10^2, 3.3) V/m. This value is close comparatively to the experimental value of $V_{exp}\approx10\,\mathrm{V}$. Also, the rather small values of $v_{ex}=v_{ey}=0.19\times10^5$ m/s (10^{-3} eV), $v_{ez}=0.9\times10^4$ m/s (2.3×10^{-4} eV) are obtained. It can be concluded that the obtained results can well explain the experimental observation

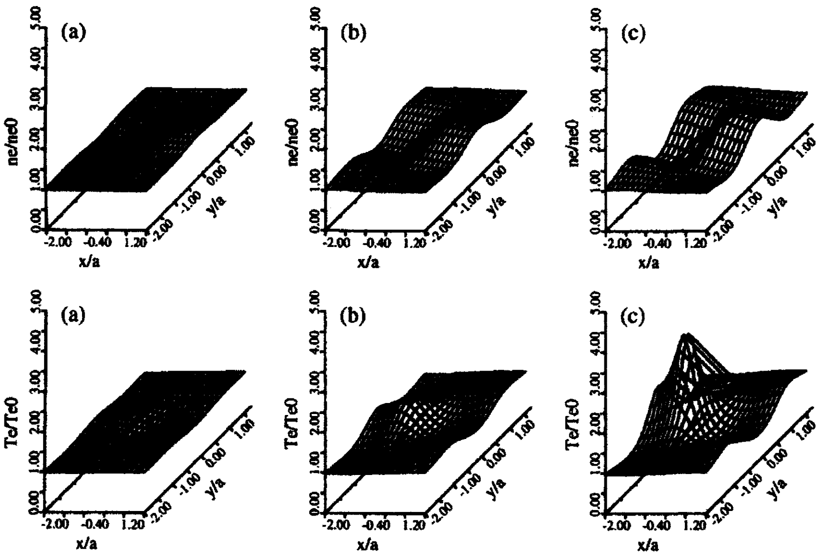

Fig. 1 Temporal evolutions of the transverse profiles of n_e / n_{e0} and T_e / T_{e0}. $D_{a0} / \gamma_N a^2 = 0$ and $\left|\gamma_k^{(e)}\right| t = 1$ for (a), 2 for (b) and 3 for (c).

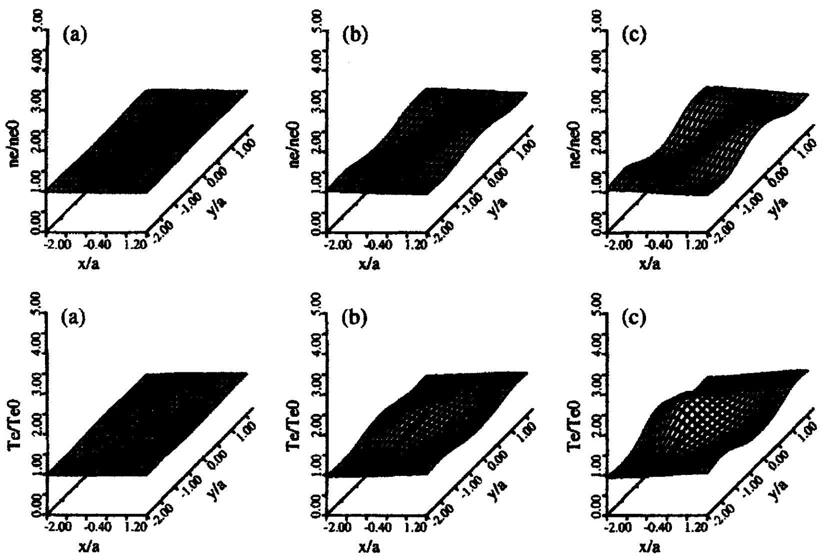

Fig. 2 Temporal evolutions of the transverse profiles of n_e / n_{e0} and T_e / T_{e0}. $D_{a0} / \gamma_N a^2 = 10^{-6}$ and $\left|\gamma_k^{(e)}\right| t = 1$ for (a), 2 for (b) and 3 for (c).

References

[1] R. Sugaya *et al.*, *Proc. Int. Cong. on Plasma Phys. Combined with the 25th EPS Conf. on Contr. Fusion and Plasma Phys.*, Praha, Czech, 1998, ECA Vol. 22C, p. 141 and p. 209.

[2] R. Sugaya *et al.*, *Proc. Int. Cong. on Phenomena in Ionized Gases*, Nagoya, Japan, 2001, Vol. 3, p. 117 and 127.

[3] R. Sugaya, J. Plasma Phys. **64**, 109 (2000); **66**, 143 (2001).

[4] R. Sugaya *et al.*, J. Plasma Fusion Res. SERIES **6**, 253 (2004).

[5] R. Sugaya *et al.*, J. Phys. Soc. Jpn. **64**, 2018 (1995).

[6] T.Maehara *et al.*, *Proc. Int. Conf. on Plasma Phys.*, Nagoya, Japan, 1996, Vol. 1, p. 426.

[7] T. Maehara *et al.*, J. Plasma Fusion Res. SERIES **4**, 322 (2001).